Characterization of Ag oxide thin films prepared by reactive RF sputtering

Yoshio Abe*, Tomoaki Hasegawa, Midori Kawamura and Katsutaka Sasaki
Department of Materials Science, Kitami Institute of Technology
165 Koen-cho, Kitami 090-8507, Japan

Abstract

Ag oxide thin films were grown on glass substrates by sputtering an Ag target in an Ar+O_2 mixed gas. Effects of O_2 flow ratio on resistivity, reflectance and transmittance of the Ag oxide films were studied. Crystal structure and chemical binding state of the films were characterized by X-ray diffraction, X-ray photoelectron spectroscopy, and scanning electron microscopy. Ag films with a resistivity of 4 μΩcm and a reflectance of 98% were obtained at O_2 flow ratios below 5%. The increase of resistivity and the decrease of reflectance were observed with increasing O_2 flow ratio due to the formation of mixed films of Ag and Ag oxide. Above an O_2 flow ratio of 40%, the transmittance of the films increased and semitransparent Ag_2O films with resistivity of an order of 10^8 Ωcm were formed.

Keywords {Ag, Ag_2O, sputtering, XRD, XPS, resistivity, reflectance, transmittance}

* Corresponding author. E-mail address: abeys@mail.kitami-it.ac.jp (Y. Abe).

1. Introduction

Recently, noble metal oxide thin films have attracted attention as materials for electronic and optical applications. For example, IrO_2 and RuO_2, which are conducting oxides with resistivities of approximately 50 μΩcm, are used as capacitor electrodes of dynamic random access memories (DRAMs) and ferroelectric RAMs (FeRAMs) [1-3] and field emitter tips [4]. Pt oxide and Pt-Rh-O_x films [5-7] are also used as the capacitor electrode of FeRAMs. Machalett *et al.* [8] reported the direct writing of an electrical conducting area by decomposing insulating PtO_2 thin films using a focused ion-beam (FIB) technique. Ag oxide and Pt oxide thin films are considered to be suitable for high-density optical disk memory technologies [9-12], because Ag and Pt nanoparticles are formed by laser irradiation to Ag oxide and Pt oxide films, and the nanoparticles are thought to be the origin of the super-resolution readout.

In oxygen plasma, noble metals react with oxygen though noble metals are considered to be chemically stable. Reactive sputtering is one of the most commonly used techniques for preparing films of noble metal oxides. Thin films of reactively sputtered IrO_2 [13-15], RuO_2 [16-18], Pt oxide [6,19,20], and Ag oxide [9,12,21-24] have been studied by many researchers. The electrical properties of IrO_2 and RuO_2 thin films have been studied extensively, however, only a few papers have been published on electrical properties of Ag oxide films prepared by reactive sputtering [24]. In this work, we studied the effects of O_2 flow ratio on the electrical resistivity of Ag oxide thin films in detail. The crystal structure, chemical binding state, surface morphology and optical properties of Ag oxide thin films were also studied.

2. Experimental

Ag and Ag oxide thin films with a thickness of approximately 150 nm were deposited by a conventional RF diode sputtering technique. The sputtering target used was an Ag metal disk (99.9% purity) with a diameter of 80mm. Corning #7059 glass (30×40 mm) was used as a substrate. Substrate temperature was varied from room temperature (RT) to 200°C. Mixed gas of Ar and oxygen was used as a sputtering gas and the oxygen flow ratio, $O_2/(Ar+O_2)$, was varied from 0% to 100%. The total gas flow rate, sputtering gas pressure and rf power were kept constant at 3.5 cm^3/min, 1 Pa and 100 W, respectively. The crystal structure and chemical binding state of the deposited films were evaluated by X-ray diffraction (XRD) with Cu Kα radiation and X-ray photoelectron spectroscopy (XPS) with Al Kα radiation, respectively. Surface XPS spectra of the films without ion sputter cleaning were measured in order to avoid decomposition of Ag oxide. Calibration of the binding energy was based on the Au $4f_{7/2}$ XPS peak (84.0 eV) from a pure Au

thin film area, which was vacuum evaporated on the Ag and Ag oxide films. Resistivity was measured by a four-point probe method for low-resistance films and by a two-terminal method for high-resistance films. Since the resistivity of Ag oxide thin films varied by over ten orders of magnitude, we used three types of sample structure for the electrical measurements. A sample with an Ag oxide film deposited on a glass substrate was used for the four-point probe method. For the two-terminal measurement, a sample with two line-shaped Au electrodes deposited on an Ag oxide film and a sample with a parallel plate capacitor structure of Au/AgO_x/Pt/glass were formed. The length and the separation width of the two line-shaped electrodes were 22 mm and 8 mm, respectively, and the electrode area of the parallel plate capacitor was 4 mm^2. The upper Au and lower Pt electrodes were deposited by vacuum evaporation and sputtering, respectively. Film thickness was estimated by multiple beam interferometry. The surface morphology of the AgO_x films was studied by scanning electron microscopy (SEM). The optical reflectance and transmittance of the films were evaluated in the wavelength region from 400 nm to 800 nm using a multichannel CCD (charge coupled device) detector.

3. Results and Discussions

First, the effect of O_2 flow ratio on crystal structure was studied. Figure 1 (a) shows XRD patterns of AgO_x films prepared at O_2 flow ratios from 0% to 100% and a substrate temperature of RT. As seen from this figure, diffraction peaks due to Ag crystals with fcc structure are observed at O_2 flow ratios of 0-30% and diffraction peaks due to cubic Ag_2O (111) [25] are observed at O_2 flow ratios of 10-30%. At O_2 flow ratios above 30%, a broad peak appeared at a diffraction angle of approximately 35°. The broad peak may be ascribed to hexagonal Ag_2O or Ag_2CO_3 [25], because Ag_2O was reported to react with CO_2 and form Ag_2CO_3 in air [23]. The intensity of the broad peak decreased with increasing O_2 flow and the diffraction peaks almost disappeared at an O_2 flow ratio of 100%. XRD patterns of the films prepared at an O_2 flow ratio of 100% and substrate temperatures of RT, 100°C and 200°C are shown in Figure 1 (b). Diffraction peaks due to cubic Ag_2O are clearly seen for the films deposited at substrate temperatures of 100°C and 200°C. This result indicates that highly crystallized Ag_2O films are grown at substrate temperatures as high as 200°C, however, thin film deposition at higher substrate temperatures was not carried out since it was reported that Ag_2O decomposes to Ag at 200-400°C [26-28]. Figure 2 shows SEM images of Ag oxide films deposited at an O_2 flow ratio of 100% and substrate temperatures of RT, 100°C and 200°C. As is clearly seen in this figure, the surface of the film deposited at RT is very smooth, however, that of the films deposited at 100°C and 200°C becomes very rough. It is supposed that

the surface migration of Ag atoms was enhanced and three-dimensional crystal growth occurred at high substrate temperatures. Therefore, measurements on XPS, electrical and optical properties of the films were carried out only for the films deposited at RT.

Figure 3 shows Ag 3d and O 1s XPS spectra of the films deposited at O_2 flow ratios of 0% and 100% at RT. The binding energy of Ag $3d_{5/2}$ was found to be 368.2 eV for a film deposited at an O_2 flow ratio of 0% and it shifted to 367.7 eV for a film deposited at an O_2 flow ratio of 100%. Since the binding energies of 368.0-368.3 eV, 367.6-367.8 eV, and 367.3-367.4 eV were reported for pure Ag, Ag_2O, and AgO, respectively [28-31], it is concluded that Ag and Ag_2O films were formed at O_2 flow ratios of 0% and 100%, respectively. In O 1s XPS spectra, a small peak at a binding energy of 531.0 eV was observed for a film deposited at an O_2 flow ratio of 0%, and double peaks at 530.8 eV and 529.2 eV were observed for a film deposited at an O_2 flow ratio of 100%. It is thought that the higher binding energy peaks at 531.0 eV and 530.8 eV are due to subsurface oxygen and Ag_2CO_3, and the lower binding energy peak at 529.2 eV is due to Ag_2O [28,29]. From the results of XRD and XPS measurements, it is found that Ag films were formed at an O_2 flow ratio of 0%, and Ag_2O began to be incorporated into the deposited films above an O_2 flow ratio of 10%. Above an O_2 flow ratio of 30%, The Ag crystals disappeared and Ag oxide films were formed.

Next, we examined the electrical and optical properties of the AgO_x films. Figure 4 shows the resistivity of the films as a function of O_2 flow ratio. A resistivity of approximately 4 μΩcm was obtained for a film deposited at an O_2 flow ratio of 0% and the resistivity increased with increasing the O_2 flow ratio. A maximum resistivity of an order of 10^8 Ωcm was obtained at an O_2 flow ratio region of 40-80%, and the resistivity decreased slightly to an order of 10^4 Ωcm at an O_2 flow ratio of 100%. The resistivity of the pure Ag films deposited at a substrate temperature of RT was slightly higher than that of bulk Ag (1.6 μΩcm). Since the crystal grain size estimated using Scherrer's equation was only 30 nm, the resistivity of the pure Ag film is thought to be increased by electron scattering at grain boundaries and crystal defects. The increase of resistivity above an O_2 flow ratio of 10% is thought to be caused by the incorporation of oxygen atoms as an impurity and the formation of semiconducting Ag_2O phase. Since Ag_2O has been reported to be a p-type semiconductor [32] with a resistivity of 7×10^8 Ωcm [33], it is confirmed that Ag_2O films were formed at O_2 flow ratios of 40-80%. The slight decrease of resistivity at an O_2 flow ratio of 100% may be caused by the incorporation of a small amount of AgO, though the existence of AgO could not be confirmed by XRD and XPS measurements since a lower resistivity of 59.3 Ωcm was reported for AgO [34]. The large difference (13 orders of magnitude) in resistivity between pure Ag

and Ag_2O films and the low decomposition temperature of Ag_2O is thought to be preferable for the FIB patterned electrode formation, similar to the case of PtO_2 thin films [8]. Furthermore, the decomposition temperature of oxide films can be controlled by the composition of Ag-Pt oxide [35].

Reflectance and transmittance spectra of the films are shown in Figures 5 (a) and (b), respectively, and the values of reflectance and transmittance at a wavelength of 600 nm are plotted as a function of O_2 flow ratio in Figure 6. A maximum reflectance of 98% was obtained at a wavelength of 600 nm for Ag films deposited at O_2 flow ratios of 0% and 5%, however, the reflectance decreased to approximately 30% above an O_2 flow ratio of 10%. The transmittance of the films was very low at O_2 flow ratios below 25%, and it began to increase at an O_2 flow ratio of 30%. For the high-transmittance films deposited above 30%, interference patterns were clearly observed in the transmittance spectra and a maximum transmittance of 80% was obtained at a wavelength of approximately 650 nm. The change of transmittance and reflectance was found to depend on the composition of the films. High-reflectance films, low-reflectance and low-transmittance films, and low-reflectance and high-transmittance films correspond to Ag films, compound films of Ag and Ag oxide, and Ag_2O films, respectively.

4. Conclusion

The effects of O_2 flow ratio on resistivity, reflectance and transmittance of Ag oxide films prepared by reactive sputtering were studied. The resistivity of pure Ag film was 4 μΩcm. With increasing O_2 flow ratio, the resistivity increased due to the formation of mixed films of Ag and Ag_2O, and semitransparent Ag_2O films with a resistivity of an order of 10^8 Ωcm were formed above an O_2 flow ratio of 40%. The optical properties of the films depended on the film composition and an abrupt decrease in reflectance was observed for the mixed films of Ag and Ag_2O, and a relatively high transmittance was obtained for the Ag_2O films.

References

[1] Vijay D P, Desu S B. J Electrochem Soc 1993;140:2640.

[2] Takemura K, Yamamichi S, Lesaicherre P-Y, Tokashiki K, Miyamoto H, Ono H, Miyasaka Y, Yoshida M. Jpn J Appl Phys 1995;34:5224.

[3] Nakamura T, Fujimori Y, Izumi N, Kamisawa A. Jpn J Appl Phys 1998;37:1325.

[4] Chalamala B R, Reuss R H, Dean K A, Sosa E, Golden D E. J Appl Phys 2002;91:6141.

[5] Lee B S, Lee J Y. Jpn J Appl Phys 1999;38:L870.

[6] Kim W S, Kim J-W, Park H-H, Lee H N. Jpn J Appl Phys 2000;39:7097.

[7] Bhatt H D, Desu S B, Vijay D P, Hwang Y S, Zhang X, Nagata M, Gill A. Appl Phys Lett 1997;71:719.

[8] Machalett F, Edinger K, Ye L, Melngailis J, Venkatesan T, Diegel M, Steenbeck K. Appl Phys Lett 2000;76:3445.

[9] Tominaga J, Haratani S, Uchiyama K, Takayama S. Jpn J Appl Phys 1992;31:2757.

[10] Kikukawa T, Tachibana A, Fuji H, Tominaga J. Jpn J Appl Phys 2003;42:1038.

[11] Kim J, Hwang I, Yoon D, Park I, Shin D, Kikukawa T, Shima T, Tominaga J. Appl Phys Lett, 2003;83:1701.

[12] Her Y-C, Lan Y-C, Hsu W-C, Tsai S-Y. Jpn J Appl Phys 2004;43:267.

[13] Cho H-J, Horii H, Hwang C S, Kim J-W, Kang C S, Lee B T, Lee S I, Koh Y B, Lee M Y. Jpn J Appl Phys 1997;36:1722.

[14] Pinnow C U, Kasko I, Dehm C, Jobst B, Seibt M, Geyer U. J Vac Sci Technol B 2001;19:1857.

[15] Ishikawa T, Abe Y, Kawamura M, Sasaki K. Jpn J Appl Phys 2003;42:213.

[16] Kolawa E, So F C T, Flick W, Zhao X-A, Pan E T-S, Nicolet M-A. Thin Solid Films 1989;173:217.

[17] Wang Q, Gladfelter W L, Evans D F, Fan Y, Franciosi A. J Vac Sci Technol A 1996;14:747.

[18] Kaga Y, Abe Y, Yanagisawa H, Sasaki K. Jpn J Appl Phys 1998;37:3457.

[19] McBride J R, Graham G W, Peters C R, Weber W H. J Appl Phys 1991;69:1596.

[20] Abe Y, Yanagisawa H, Sasaki K. Jpn J Appl Phys 1998;37:4482.

[21] Rizk A, Maker L N, Rizk N S, Shinoda R. Vacuum 1990;40:285.

[22] Büchel D, Tominaga J, Fukaya T, Atoda N. J Magn Soc Japan. 2001;25:240.

[23] Djokic S S, Burrell R E, Le N, Field D J. J Electrochem Soc 2001;148:C191.

[24] Barik U K, Srinivasan S, Nagendra C L, Subrahmanyam A. Thin Solid Films 2003;429:129.

[25] JCPDS- International Centre of Diffraction Data. PDF-s Database CD-ROM Version 2000.

Nos. 41-1104, 19-1155, and 26-339.
[26] Lide D R ed. Handbook of Chemistry and Physics 84th ed. Boca Raton: CRC Press, 2003. p.4-83.
[27] Pettinger B, Bao X, Wilcock I, Muhler M, Schlögl R, Ertl G. Angew Chem Int Ed Engl 1994;33:85.
[28] Weaver J F, Hoflund G B. J Phys Chem 1994;98:8519.
[29] Gaarenstroom S W, Winograd N. J Chem Phys 1977;67:3500.
[30] Tjeng L H, Meinders M B J, van Elp J, Ghijsen J, Sawatzky G A. Phys Rev B 1990;41:3190.
[31] Moulder J F, Stickle W F, Sobol P E, Bomben K D. Handbook of X-ray Photoelectron Spectroscopy. Eden Prairie: Parkin-Elmer, 1992. p.172.
[32] Talukdar M I, Baker E H. Solid State Communications 1969;7:309.
[33] Cahan B D, Ockerman J B, Amlie R F, Ruetshi P. J Electrochem Soc 1960;107:725.
[34] Tvarusko A. J Electrochem Soc 1968;115:1105.
[35] Shima T, Tominaga J. Thin Solid Films 2003;425:31.

Figure captions

Fig. 1. XRD patterns of AgO_x films deposited at various O_2 flow ratios and substrate temperatures. (a): substrate temperature of RT. (b): O_2 flow ratio of 100%.

Fig. 2. Surface SEM images of AgO_x films deposited at an O_2 flow ratio of 100% and substrate temperatures of (a) RT, (b) 100°C and (c) 200°C.

Fig. 3. Ag 3d and O 1s XPS spectra of AgO_x films deposited at O_2 flow ratios of 0% and 100%, and at a substrate temperature of RT.

Fig. 4. Resistivity of AgO_x films deposited at a substrate temperature of RT as a function of O_2 flow ratio.

Fig. 5. Reflectance and transmittance spectra of AgO_x films deposited at various O_2 flow ratios and at a substrate temperature of RT.

Fig. 6. Reflectance and transmittance of AgO_x films deposited at a substrate temperature of RT as a function of O_2 flow ratio. The wavelength λ used for the measurement was 600 nm.

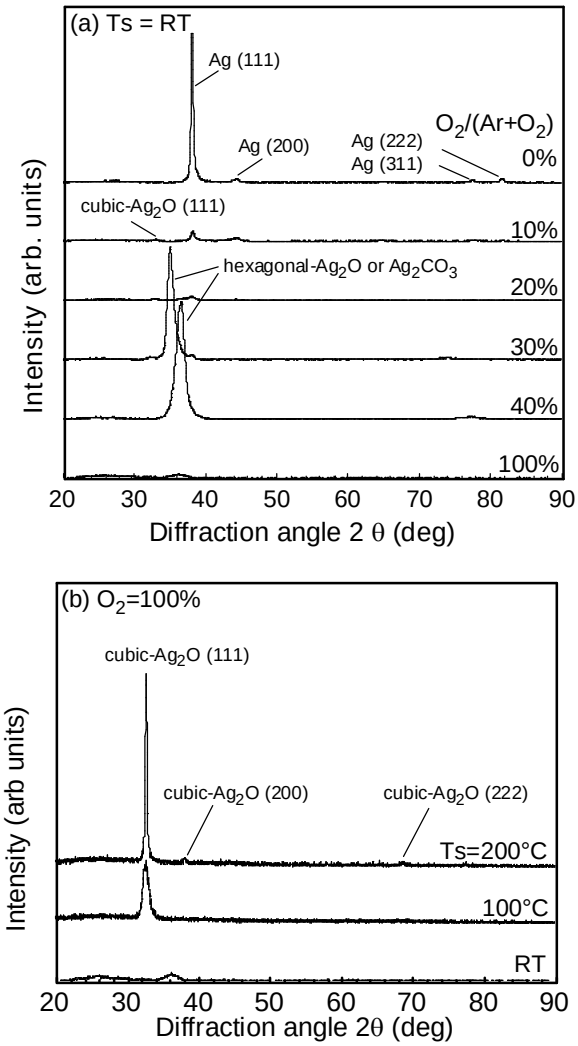
(a) Ts = RT
Ag (111)
Ag (200)
Ag (222)
Ag (311)
O2/(Ar+O2)
0%
cubic-Ag2O (111)
10%
hexagonal-Ag2O or Ag2CO3
20%
30%
40%
100%
Intensity (arb. units)
20 30 40 50 60 70 80 90
Diffraction angle 2 θ (deg)
(b) O2=100%
cubic-Ag2O (111)
cubic-Ag2O (200)
cubic-Ag2O (222)
Ts=200°C
100°C
RT
Intensity (arb units)
20 30 40 50 60 70 80 90
Diffraction angle 2θ (deg)

Fig. 1

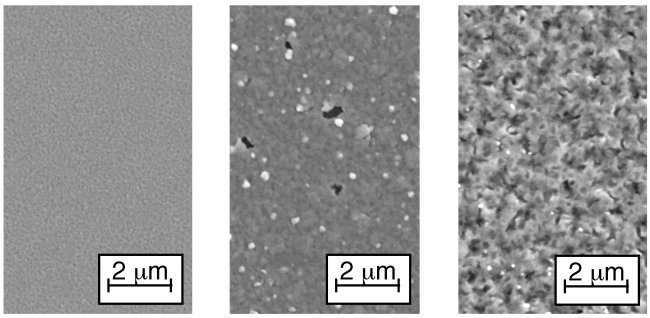

(a) Ts=RT (b) Ts=100°C (c) Ts=200°C

Fig. 2

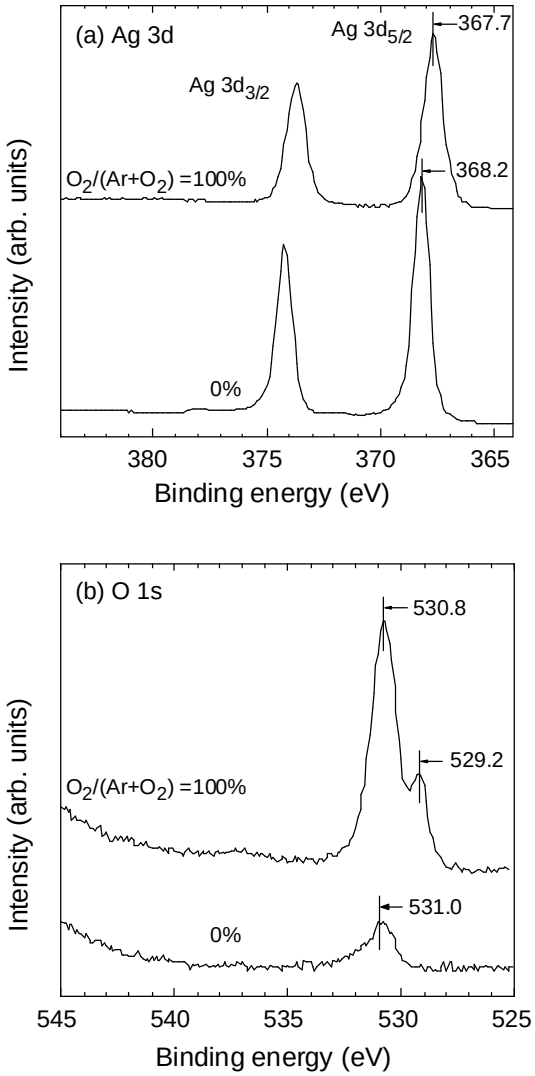
(a) Ag 3d
Ag 3d5/2
367.7
Ag 3d3/2
O2/(Ar+O2) =100%
368.2
0%
Intensity (arb. units)
380
375
370
365
Binding energy (eV)
(b) O 1s
530.8
529.2
O2/(Ar+O2) =100%
531.0
0%
Intensity (arb. units)
545
540
535
530
525
Binding energy (eV)

Fig. 3

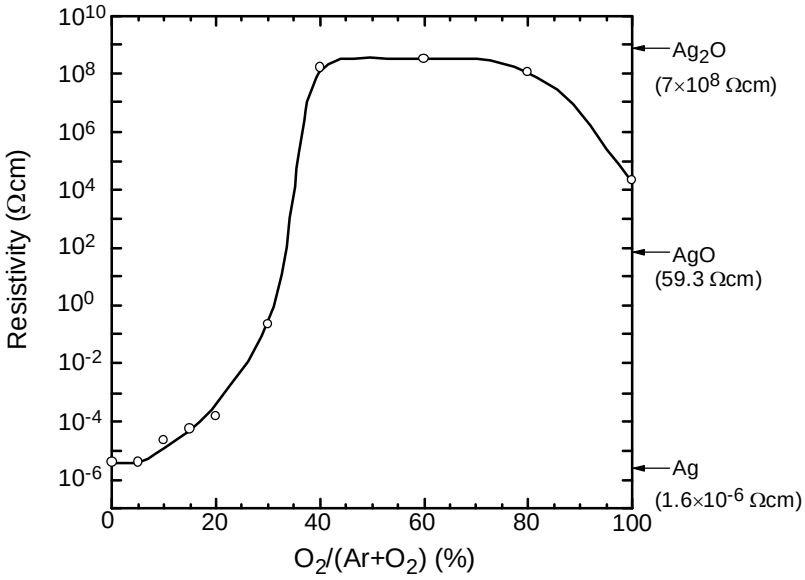
Resistivity (Ωcm)
10^10
10^8
10^6
10^4
10^2
10^0
10^-2
10^-4
10^-6
0
20
40
60
80
100
O2/(Ar+O2) (%)
Ag2O
(7×10^8 Ωcm)
AgO
(59.3 Ωcm)
Ag
(1.6×10^-6 Ωcm)

Fig. 4

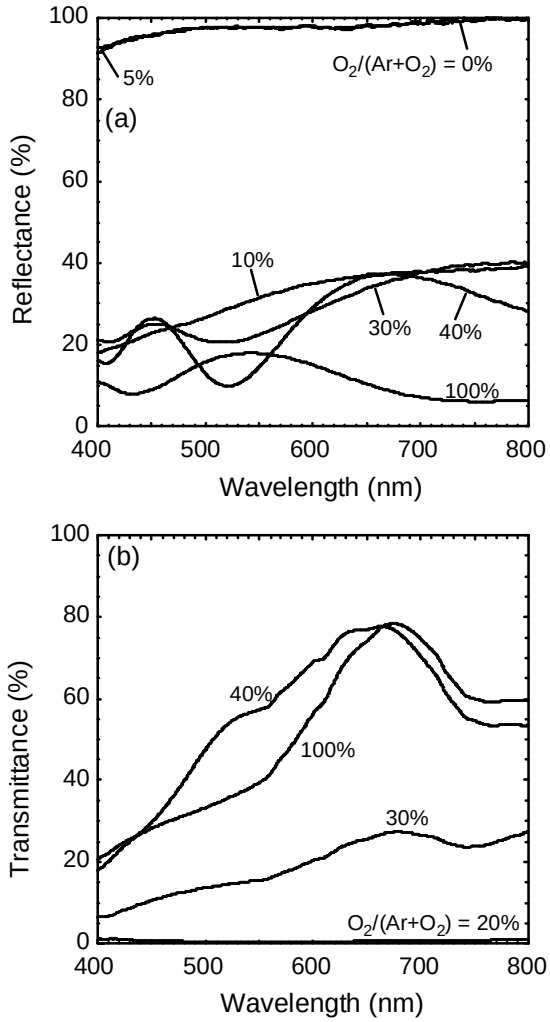
(a)
Reflectance (%)
Wavelength (nm)
5%
$O_2/(Ar+O_2)$ = 0%
10%
30%
40%
100%
(b)
Transmittance (%)
Wavelength (nm)
40%
100%
30%
$O_2/(Ar+O_2)$ = 20%

Fig. 5

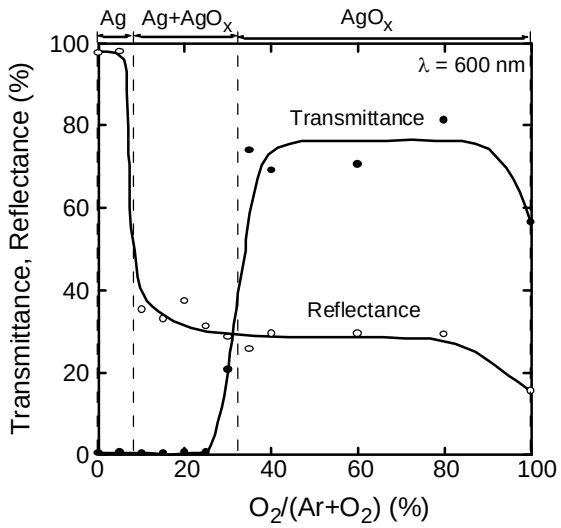
Ag
Ag+AgO$_x$
AgO$_x$
λ = 600 nm
Transmittance
Reflectance
Transmittance, Reflectance (%)
O$_2$/(Ar+O$_2$) (%)
0
20
40
60
80
100

Fig. 6